THERMAL SYSTEM MODELING FOR LUNAR AND MARTIAN SURFACE REGENERATIVE FUEL CELL SYSTEMS

Ryan P. Gilligan, Phillip J. Smith, Ian J. Jakupca, William R. Bennet, Monica C. Guzik, James Fincannon
National Aeronautics and Space Administration, John H. Glenn Research Center, Cleveland, OH, 44135

ABSTRACT

The Advanced Exploration Systems (AES) Advanced Modular Power Systems (AMPS) Project is investigating different power systems for various lunar and Martian mission concepts. The AMPS Fuel Cell (FC) team has created two system-level models to evaluate the performance of regenerative fuel cell (RFC) systems employing different fuel cell chemistries. Proton Exchange Membrane fuel cells PEMFCs contain a polymer electrolyte membrane that separates the hydrogen and oxygen cavities and conducts hydrogen cations (protons) across the cell. Solid Oxide fuel cells (SOFCs) operate at high temperatures, using a zirconia-based solid ceramic electrolyte to conduct oxygen anions across the cell. The purpose of the modeling effort is to down select one fuel cell chemistry for a more detailed design effort. Figures of merit include the system mass, volume, round trip efficiency, and electrolyzer charge power required. PEMFCs operate at around 60 ºC versus SOFCs which operate at temperatures greater than 700 ºC. Due to the drastically different operating temperatures of the two chemistries the thermal control systems (TCS) differ. The PEM TCS is less complex and is characterized by a single pump cooling loop that uses deionized water coolant and rejects heat generated by the system to the environment via a radiator. The solid oxide TCS has its own unique challenges including the requirement to reject high quality heat and to condense the steam produced in the reaction. This paper discusses the modeling of thermal control systems for an extraterrestrial RFC that utilizes either a PEM or solid oxide fuel cell.

INTRODUCTION

As the National Aeronautics and Space Administration (NASA) continues to define its goals for surface exploration beyond Earth, the need persists for consistent and reliable power systems to meet the demands of both manned and large-scale robotic missions. Regenerative fuel cell (RFC) systems are energy storage devices and a viable option as a power system. A fuel cell facilitates an electrochemical reaction to provide electrical power both to the RFC system and to an external customer. Multiple fuel cells are assembled electrically in series to build a fuel cell stack. The byproducts of a fuel cell that uses hydrogen and oxygen reactants are water and heat. Similarly to batteries an RFC must recharge and this is achieved via electrolysis. An electrolyzer requires power from an external source and electrochemically converts the water produced by the fuel cell back into hydrogen and oxygen gas. The Advanced Exploration Systems (AES) Advanced Modular Power Systems (AMPS) project is investigating different power and energy

storage systems for selected lunar and Martian mission concepts including RFCs. The surface power system concept utilizes solar arrays to provide the customer with power during the day and to power an electrolyzer to recharge the RFC. When solar power is not available, such as during the night time or during eclipses, the fuel cell stack would satisfy the power demands of the customer. The AMPS Fuel Cell (FC) team has created two system-level models in Microsoft Excel to evaluate the performance of regenerative fuel cell systems employing different fuel cell chemistries. This paper discusses the thermal modeling considerations for each system.

Proton Exchange Membrane (PEM) fuel cells utilize a polymer electrolyte membrane that separates the hydrogen and oxygen cavities and conducts protons across the cell. Two protons and two electrons are created from catalytically breaking the covalent bond in one hydrogen molecule. The electrons flow through the electronic circuit thus providing power to the load. Platinum catalysts are typically used and are susceptible to poisoning by contaminants, such as sulfur or carbon monoxide, so the PEMFC has stringent reactant purity requirements. Poisoning of the fuel cell is defined as irreversible damage that causes reduced performance. PEMFCs run most efficiently on pure hydrogen and oxygen gas. PEMFCs operate at moderate temperatures, 60 ºC to 80 ºC, and pressure ranges, 12 psia to 120 psia. “Because the cell separator is a polymer film and the cell operates at relatively low temperatures, issues such as sealing, assembly, and handling are less complex than most other fuel cells” [1]. For the chemical reaction to persist, the product water must continuously be removed from the stack. In terrestrial flow through fuel cell stacks a greater than stoichiometric quantity of air is flown through the stack to remove the product water that is created in the oxygen cavity of the fuel cell. Some PEMFC designs can operate in a non-flow-through (NFT) mode with only stoichiometric quantities of reactant supplied to the stack. NFT FCs employ advanced water removal techniques using differential pressures and surface forces to remove product water from the oxygen cavity. Utilizing a NFT fuel cell stack can simplify the system by removing a recirculation pump from the design.

Solid Oxide fuel cells (SOFCs) operate at high temperatures (600-1000 ºC), using a zirconia-based solid ceramic electrolyte to conduct oxygen anions across the cell. SOFCs are less susceptible to poisoning than PEMFCs and can operate on a variety of fuels including reformed hydrocarbons. The high operating temperature allows for highly efficient conversion of chemical energy to electrical power. However, the high temperature also the design challenge of finding suitable materials for sealing; this still plagues SOFCs which have much higher external leak rates than PEMFCs. Another difficulty in SOFC design is finding materials for the anode, cathode, and other parts of the fuel cell that have similar coefficients of thermal expansion (CTE). Any mismatch in CTE adds thermally-induced mechanical stresses whenever a thermal gradient exists within a solid oxide stack. The high operating temperature also complicates the thermal control system. In ground based systems, the high quality heat from a SOFC could be used in a bottoming cycle [4]. For reliability purposes this was not considered for the lunar or Martian RFCs as it would add undue complexity to an already complex system.

PEMFC THERMAL SYSTEM MODELING

The piping and instrumentation diagram (P&ID) for a notional PEM RFC system is shown in Figure 1. The modeling effort focused solely on the RFC and neglected the solar array design and power management and distribution (PMAD) system. Note one difference between the Figure 1 and the system modeled is that three fuel cells and three electrolyzers were used to meet the total power and reactant generation demand in the Excel model to address stack-level redundancy requirements. The FC and electrolyzer (EZ) stacks were sized so that if one stack were to fail the remaining two could still meet the peak electrical loads. The power requirement for the trade study was to deliver 10 kW to the PMAD system which would then deliver power to the customer.

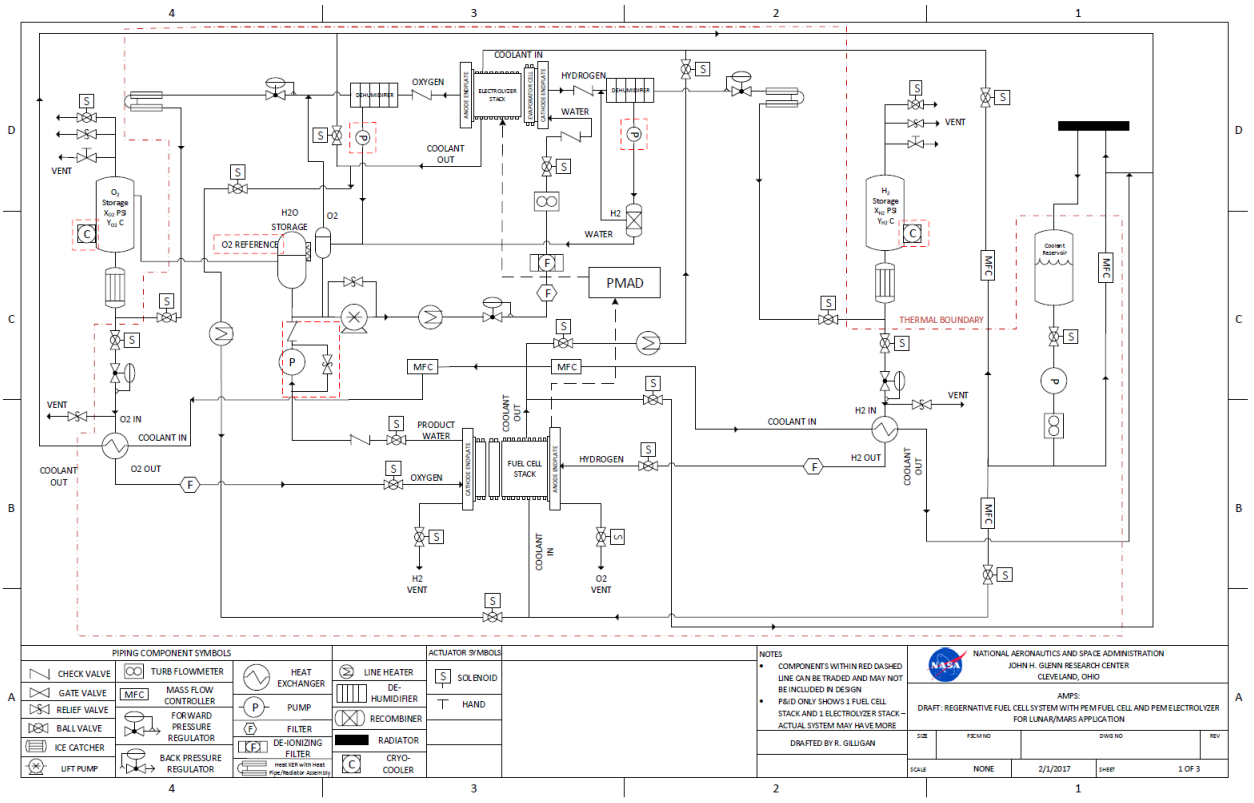

Figure 1. Notional Proton Exchange Membrane (PEM) Fuel Cell Piping and Instrumentation Diagram (P&ID) for an extraterrestrial regenerative fuel cell (RFC) system.

The PEM RFC has three principal thermal requirements. The first requirement is to reject the waste heat produced by the fuel cells and electrolyzers during operation. The maximum fuel cell heat load is 7.6 kW of waste heat for 10.2 kW net electrical power generation. The second requirement is to minimize thermal cycling of the fuel cell and electrolyzer. Though not nearly as extreme as thermal cycling for SOFCs, going through many cycles of temperature changes from

the minimum allowable PEM temperature (20 ^{0}C) to operational temperature (60 ^{0}C) leads to mechanical stress cycling which may result in delamination of the polymer membrane and catalyst [2]. The third requirement relates to keeping the liquid water in various parts of the system from freezing during all aspects of the mission from launch to decommissioning. For example the electrolyte in PEM stacks is hydrated with liquid water and the ice crystals created when water freezes would stress and damage the polymer within the membrane electrode assembly. Also the coolant used in the system is water which must obviously be kept in the liquid state.

Traditional PEM fuel cell systems have coolant flow passages built into the bipolar plate structure to allow the heat from the reaction to be uniformly removed from stack via a liquid coolant. Due to the high heat capacity and poor electrical conductivity, a conventional coolant is deionized water which was therefore chosen as the baseline for this preliminary trade study. For the preliminary trade this was used as the baseline coolant. The model contains a database of thermodynamic and physical properties for water. The coolant system contains a coolant reservoir, pump, flow meter, various solenoid valves, mass flow controllers, and a radiator. During fuel cell operation, the coolant is routed from the pump to fuel cell and the majority of the flow is then routed directly to the electrolyzer before running through the radiator for heat rejection. This concept allows the waste heat produced by the fuel cell to be used to keep the electrolyzer near its operational temperature while it is in a standby mode, thus satisfying the second thermal requirement.

In order to calculate the efficiency of the RFC system the parasitic loads must be determined. The primary parasitic load of the coolant system is the pump. The required mass flow rate to reject the waste heat generated by the fuel cell, Q_{FC}, is calculated using Equation 1 and solving for $\dot{m}_{coolant}$.

$$Q_{FC} = \dot{m}_{coolant} c_p \Delta T \qquad (1)$$

The waste heat generated by the fuel cell is in W, $\dot{m}_{coolant}$ is the mass flow rate of coolant in kg/s, c_p is the specific heat at constant pressure of the coolant in J/kg-K, and ΔT is the desired fuel cell temperature differential in K. This RFC model is intended to be a high-level system model so instead of considering various intricate geometries and calculating the resulting heat transfer, ΔT is an input for the model and given a baseline value. Data on PEM fuel cells tested at NASA Glenn Research Center suggests a range of 2 ^{0}C to 10 ^{0}C increase in coolant temperature from inlet to outlet. For the stacks in this RFC model a ΔT value of 5 ^{0}C was chosen. Equation 1 can also be used to calculate the coolant flow rate required to reject waste heat during electrolyzer operation.

The required flow rate was used to size a pump for the coolant system. The ideal power, $\dot{W}_{ideal}$, required to pressurize a fluid from a lower pressure to a higher pressure for a given flow rate is described by Equation 2.

$$\dot{W}_{ideal} = \frac{\dot{m}\Delta P}{\rho} \qquad (2)$$

ΔP is the change in pressure of the fluid through the pump in Pa, $\dot{m}$ is the mass flow rate in kg/s, and ρ is the density of the fluid in kg/m^3. A detailed pressure drop analysis was not performed for this preliminary trade as it was not going to affect the selection of solid oxide or PEM technology; instead a pressure drop through system components including valves, heat exchangers, fuel cell, and electrolyzers was assumed and the cumulative loss was used to estimate the operating pressure of the system. The density of the deionized water coolant was pulled from a lookup table based on the temperature of the liquid. The actual pump power required, $\dot{W}_{actual}$, is calculated by assuming a pump efficiency, η_{pump}.

$$\dot{W}_{actual} = \dot{W}_{ideal}\eta_{pump} \quad (3)$$

The RFC mass is also one of the key model outputs so a mass estimate of the coolant system must also be obtained. Data on several commercial off the shelf pumps was used to estimate the mass of the pump. A pump mass vs maximum flow plot was generated with the data on 4 centrifugal pumps. The flow requirement calculated from Equation 1 plus margin was plugged into the best fit curve to estimate the pump mass. Figure 2 shows the data points and linear best fit curve.

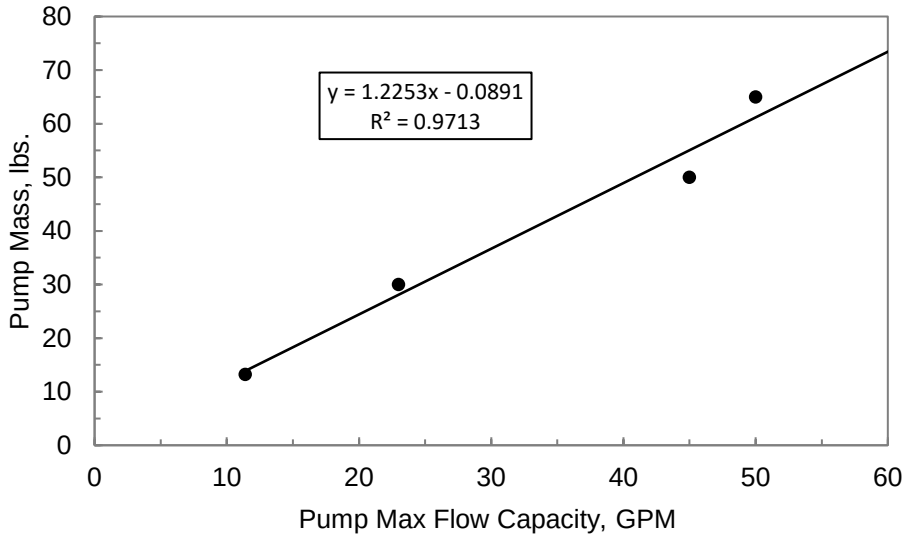

Figure 2 – Pump maximum flow capacity versus pump mass for centrifugal pump with best curve fit (solid line).

A fraction of the coolant flow leaving the fuel cell goes to heat exchangers that preheat the reactants. The reactants are stored at ambient temperature which varies by location but can be as low as -175 ^{0}C at the lunar south pole during an eclipse. A liquid gas heat exchanger is used to preheat the reactant to the required temperature for operation (minimum 15 ^{0}C). Equation 1 is used to calculate the heat that must be transferred to the reactants to raise them to 15 ^{0}C, except that the mass flow $\dot{m}$, specific heat C_p and temperature differential ΔT of the reactants is used instead of the coolant. Mass flow controllers are used to regulate this flow as required. The Log Mean Temperature Difference (LMTD) is often used when sizing heat exchangers [3].

$$LMTD = \frac{\Delta T_1 - \Delta T_2}{ln(\frac{\Delta T_1}{\Delta T_2})} \quad (4)$$

For simplicity counter flow heat exchangers were chosen. For a counter flow heat exchanger, $\Delta T_2 = T_{h,i} - T_{c,o}$ and $\Delta T_1 = T_{h,o} - T_{c,i}$ where the subscript *h* represents the hot fluid (the coolant) and the subscript *c* is for the cold fluid (the reactant gas), the subscript *i* is for inlet and *o* is for outlet. The coolant ΔT through the heat exchanger is an additional input to the model; it was assumed to be 2 K for the first round of trades. The LMTD is used to describe the heat transfer, *Q*, in a heat exchanger as shown in Equation 5.

$$Q = UA * LMTD \quad (5)$$

In Equation 5, *U* is the overall heat transfer coefficient in W/m^2-K and *A* is the heat transfer area in m^2. By assuming a temperature drop of the liquid water coolant through the heat exchanger, the LMTD can be calculated using Equation 4. Table 1 consists of values for the overall heat transfer coefficient for heat exchangers with various hot and cold fluids in shell and tube heat exchangers [5]. For gases near atmospheric pressure exchanging heat with water an average value of 20 W/m^2-K was selected. Knowing *Q*, *U*, and *LMTD* allows for the heat transfer area, *A*, required to be calculated using Equation 5.

Table 1. Typical Values for Overall Heat Transfer Coefficient.

Hot Fluid	Cold Fluid	Overall Heat Transfer Coefficient Range		
		Low W/m^2.K	High W/m^2.K	Average W/m^2.K
Water	Water	800	1500	1150
Organic solvents	Organic Solvents	100	300	200
Light oils	Light oils	100	400	250
Heavy oils	Heavy oils	50	300	175
Reduced crude	Flashed crude	35	150	92.5
Regenerated DEA	Foul DEA	450	650	550
Gases (p = atm)	Gases (p = atm)	5	35	20
Gases (p = 200 bar)	Gases (p = 200 bar)	100	300	200
Organic solvents	Water	250	750	500
Light oils	Water	350	700	525
Heavy oils	Water	60	300	180
Reduced crude	Water	75	200	137.5
Gases (p = atm)	Water	5	35	20

Gases (p = 200 bar)	Water	150	400	275
Organic solvents	Brine	150	500	325
Water	Brine	600	1200	900
Gases	Brine	15	250	132.5

Table 2 lists the ratio of heat exchanger weight to heat transfer area required for different carbon steel heat exchangers [6]. This information is normalized to include heat exchangers of various materials by dividing the density of the heat exchanger material by the density of carbon steel. Thus using Table 2 and the heat transfer area *A*, the mass of the heat exchanger in kg, m_{HX}, is estimated.

$$m_{HX} = A(WR)(\frac{\rho_{HX}}{\rho_{carbon\ steel}}) \quad (6)$$

WR is the weight ratio from Table 2 for the given type of heat exchanger in kg-force/m^2, ρ_{HX} is the density of the heat exchanger material, and $\rho_{carbonsteel}$ is the density of carbon steel. The model has a database of common pressure vessel and heat exchanger materials that the user can select from for the heat exchanger.

Table 2. Weight to heat transfer area ratio for carbon steel heat exchangers.

Heat Exchanger Type	Weight ratio for carbon steel
	kg/m^2
Liquid to liquid shell and tube	39.1
Double pipe, finned tube	24.4
Liquid to air banks of finned tubes	4.9
Plate coils	12.7
Steam condenser	29.3

Once the heat transfer area of the heat exchanger is known, the heat exchanger dimensions can also be calculated. Due to packaging volume constraints the heat exchanger considered could not be one very long purely counter flow heat exchanger. Multiple tubes and passes within the heat exchanger would be required to reduce the footprint of the heat exchanger. However, it is difficult to construct a true counter flow heat exchanger that has multiple fluid passes [6]. In practice, a combination of a counter flow and cross flow type heat exchanger would simplify manufacturing. "In this type of heat exchanger, the headers in which the fluid enters and leaves the heat exchanger operate in a cross-flow manner whereas the inner core operates in a counter-

flow manner. In general, the performance of this type of heat exchanger is better than a cross-flow design but not as effective as a pure counter-flow one" [6]. The number of tubes, n_t, and the number of passes, n_p, and out diameter of the tubes, d, are inputs to the model and can be varied to achieve a desired length, width, and height of the heat exchanger. The length of the heat exchanger, L_{HX}, is calculated using Equation 7.

$$L_{HX} = \frac{A}{\pi d n_p n_t} \quad (7)$$

The thickness of the heat exchanger, t_{HX}, is dependent on the number of stacked tubes, n_s, in the thickness direction.

$$t_{HX} = d(2n_s + 1) \quad (8)$$

The width, w_{HX}, is dependent on the number of tubes, number of passes, and the number of stacked tubes [6].

$$w_{HX} = d(\frac{2n_t n_p}{n_s} + 1) \quad (9)$$

Thus by varying n_t, n_s, and n_p the dimensions of the heat exchanger can be manipulated to a certain extent to accommodate the RFC design.

The heat generated by the fuel cell and electrolyzer is rejected to the ambient environment via a two sided radiator. The radiator design is based off the external DDCU heat pipe radiator design used for the International Space Station [7]. The radiator consists of two parts, a baseplate which is a heat exchanger that transfers heat from the warm coolant to the second part, the radiator, via heat pipes. The working fluid in the heat pipes is ammonia which limits the baseplate temperature range from – 30 ^{0}C to 65 ^{0}C. Inputs to the radiator sizing model include the maximum sink (ambient) temperature, maximum baseplate temperature, maximum baseplate – radiator ΔT, heat to reject, interface areal energy, view factor, and emissivity. The maximum sink temperature is determined by the ambient environment, and average daytime and night time temperatures were determined for each location. The fuel cell operates during the night so the night time sink temperature was used for the fuel cell heat load and the daytime sink temperature was used for the electrolyzer heat load. The model chooses the larger radiator based on the requirements of the electrolyzer and fuel cell. The maximum baseplate temperature is the maximum fuel cell operating temperature of 60 ^{0}C. The baseplate – radiator ΔT is a design factor and was assumed to be 4 ^{0}C. This would be determined by the effectiveness of the baseplate heat exchanger. It's assumed that there are no obstructions between the radiator and the sink so the view factor, F, is 1. The color of the radiator surface is white so the emissivity, ε, is 0.92. A detailed design of this heat exchanger was not performed. It was assumed that a thermostatic valve would regulate flow to the radiator to achieve a desired temperature in the coolant reservoir which is essentially the coolant inlet temperature to the fuel cell.

$$A_R = \frac{Q}{2\sigma\varepsilon F[(T_{BP} - \Delta T_{BP-R})^4 - T_{sink}^4]} \quad (10)$$

In Equation 10 A_R is the required radiator area in m^2, Q is the waste heat produced by the fuel cell or electrolyzer in W, σ is the Stefan-Boltzman constant $5.67x10^{-8}$ W/m^2-K^4, T_{BP} is the temperature of the baseplate in K, ΔT_{BP-R} is the temperature difference between the baseplate and the radiator, and T_{sink} is the sink temperature in K [7]. The radiator area required to reject 7.6 kW is very large, on the order of several meters squared. The radiator is assumed to be 2 cm thick so the mass of the radiator can be calculated. A lightweight carbon-carbon material was chosen for the radiator.

$$m_R = A_R t_R \rho_R \tag{11}$$

m_R is the mass of the radiator, t_R is the thickness of the radiator, and ρ_R is the density of the radiator material. On the RFC side, a baseplate and other mounting hardware must be sized to attach a radiator coldplate and radiator. Because the radiator design is not intended to be replaceable, this reduces the amount of mounting hardware for the coldplate-radiator assembly. The baseplate and other mounting hardware mass is derived from the as built external DDCU hardware mass for the area of the box which had the radiator attached to it. The mass of the as-built DDCU baseplate and mounting hardware using carbon-carbon materials is 8.9 kg. The area on the box which had the radiator attached to it was 0.72 m by 0.61 m. Thus the mass per unit area for the baseplate and mounting hardware mass is 8.9 kg/(0.72m*0.61m)=20.3 kg/m^2. The area of the desired baseplate is based on the amount of power that could be transferred in the as-built external DDCU. This value was 833 W/m^2. The baseplate and mounting hardware mass then is 20.3 kg/m^2*(desired heat rejection in W)/833 W/m^2. The coldplate mass is simply the radiator interface area times the carbon-carbon material areal mass (13.6 kg/m^2). Thus, the coldplate mass is 13.6 kg/m^2*desired heat rejection_watts/833 W/m^2.

A significant portion of the coolant system mass comes from the coolant. The coolant reservoir was sized based on residency time, or average time that a given amount of coolant will remain in the reservoir before being recirculated through the system. The maximum flow requirement determined by Equation 1 times the desired residency time determined the volume of the coolant vessel. The coolant volume is cylindrical so once the volume V is known, a length to diameter, L/D, ratio must be specified to calculate the length and diameter of the vessel.

$$D = 2\left(\frac{V}{2\pi\left(L/D - 1/3\right)}\right)^{1/3} \tag{12}$$

Once the inside diameter is determined the length of the vessel is easily calculated by multiplying by L/D. The tank walls were sized according to the ASME Section VIII Division 1 Boiler and Pressure Vessel Code [8].

$$t_{cyl} = \frac{PR_{cyl}}{SE - 0.6P} \tag{13}$$

P is the internal design pressure of the vessel, R_{cyl} is the radius of the cylinder, S is the maximum allowable stress value, E is the joint efficiency , and t_{cyl} is the thickness of the cylindrical section of the tank. The safety factor the tank is two so the maximum allowable stress is half of the yield stress of the tank material. In order to use Equation 13, the joint efficiency must be assumed to

be one for both circumferential and longitudinal joints. The thickness of the hemispherical heads of the tank are calculated through Equation 14 [8]. It is assumed that the radius of the spherical head is the same as the radius of the cylinder.

$$t_{head} = \frac{PR_{cyl}}{2SE - 0.2P} \quad (14)$$

Once all the dimensions of the coolant tank are established, the mass of the coolant tank is calculated by multiplying the density of the chosen material by the volume of the material. A 316 stainless steel tank was chosen for this model to maximize coolant water resistivity. The total coolant volume is the volume of coolant in the tank plus the coolant in the tubes, assumed to be 1/5 of the coolant in the tank. The mass of the coolant can then be calculated by multiplying its volume by the liquid density.

The coolant system described allows the waste heat produced by the system to be rejected to the ambient environment, thus satisfying the first thermal requirement. The third requirement relates to keeping the water coolant in a liquid state and also to keep water in the fuel cell and electrolyzer membranes from freezing. In Figure 1, the majority of the system, excluding the hydrogen and oxygen tanks, is enclosed in a red dashed line which resembles the thermal barrier of the system. This barrier is intended to provide a stable ambient temperature around 20 °C for the components inside. The proposed concept for the barrier is a metal cylinder or dome that encloses the fuel cell, electrolyzer, coolant reservoir, fluid lines, pumps, valves, etcetera. The cylinder would be insulated with multi-layer insulation on the outside surface. Electric heaters inside the metal would provide heat to the structure when heat is needed such as during standy modes or when the system is in transit. Additionally, cooling may be needed in some locations so coolant lines could be in thermal contact with the structure to remove heat. The model currently only considers the mass and volume of an aluminum enclosure around the system. A more detailed design of how to maintain this boundary temperature has been identified as forward work for the next stage of modeling. The radiated heat coming from the fuel cell and electrolyzer are accounted for as heat into this system; while radiation from the thermal boundary to the ambient environment is accounted for as heat leaving the system. It is assumed that the RFC is deployed on a lander and that the lander shields the RFC from solar flux.

This thermal system concept as described is able to meet the three primary thermal requirements for the PEM system. The mass and power draw of the coolant system feed into the main outputs of the RFC model to determine the system mass, volume, and round trip efficiency.

SOFC THERMAL SYSTEM MODELING

A SOFC RFC system shares the same thermal requirements, but has a different design to meet those requirements due to the high operating temperature of the SOFC. Figure 3 shows a conceptual SOFC RFC design. Note the RFC system for the trade study utilizes a SOFC but a PEM electrolyzer. Solid oxide electrolyzers (SOEZ) were eliminated from the trade study because current state of the art SOEZs are only capable of generating pressures up to 120 psia and also have leak rates significantly higher than that of PEM technologies. Including the necessary hardware to mechanically pressurize the SOEZ products to the required storage pressure induced unacceptable efficiency, reliability, and mass penalties.

The first thermal requirement is to reject the heat generated by the SOFC and PEM EZ. The same liquid water coolant scheme as was described previously can be applied for the PEM EZ heat rejected. The high operating temperature allows the electrochemical reaction of SOFCs to be more efficient than their PEM counterparts so for a constant 10 kW of power generation a SOFC will generate less heat than a PEMFC, around 3.5 kW of heat for this trade study. Although the total heat to reject is less for SOFCs, the heat to be rejected is high quality heat which makes a liquid water cooling loop through the fuel cell impossible. The SOFC requires four heat exchangers and two high temperature blowers to recirculate unreacted gas, one for hydrogen and one for oxygen. The first heat exchanger is a recuperative heat exchanger used to raise the temperature of the hydrogen or oxygen entering the fuel cell from the hot effluent from the stack. Small electric heaters are used to raise the inlet gas from the exit of the recuperative heat exchanger to the stack operating temperature.

In PEM systems, the product water is generated in the oxygen cavity. For solid oxide systems, steam is generated in the hydrogen cavity. The PEM electrolyzer requires liquid water so the steam exiting the SOFC must be condensed prior to storage. The second heat exchanger in the hydrogen system uses a liquid water cooling loop to condense the steam to liquid water for storage.

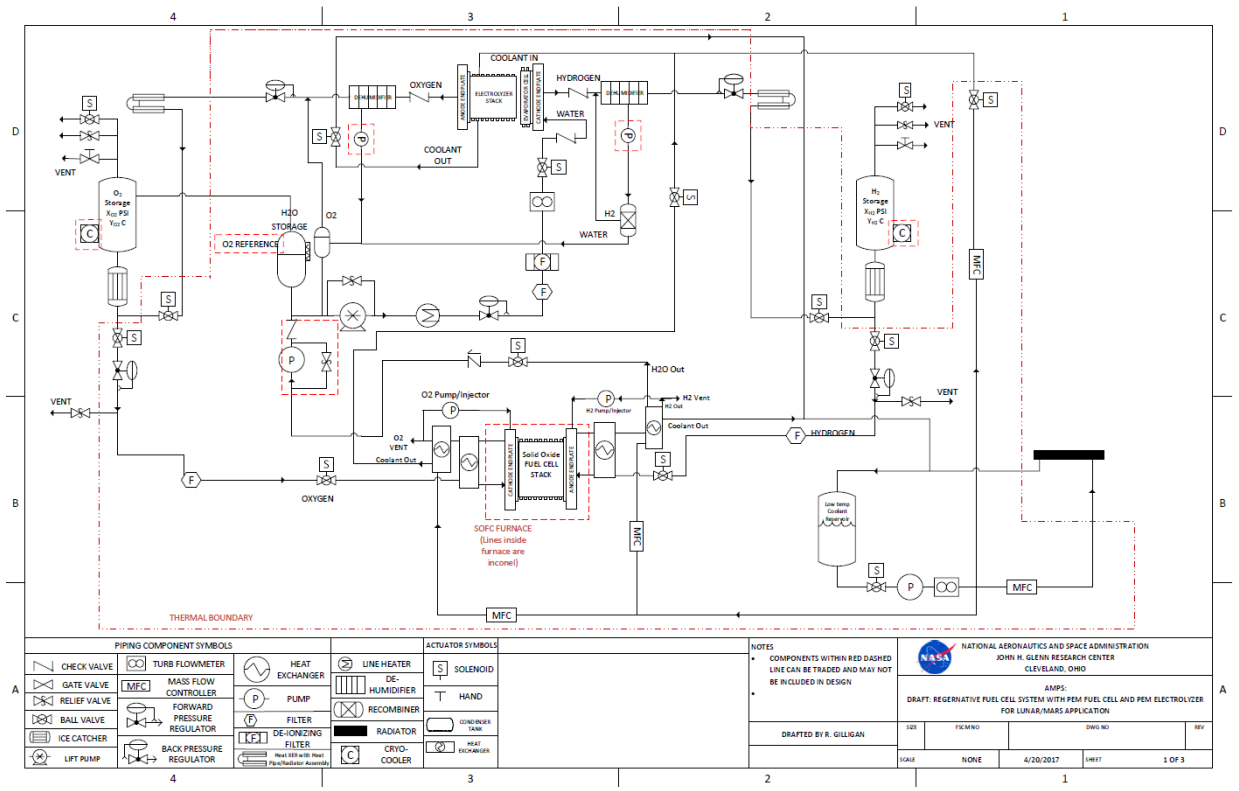

Figure 3. Piping and Instrumentation Diagram (P&ID) of conceptual Regenerative Fuel Cell system that uses a solid oxide fuel cell and proton exchange membrane electrolyzer.

The second heat exchanger in the oxygen system is used to cool the gas exit stream and remove heat generated by the system. In SOFC systems the waste heat is removed by flowing excess reactant through the stack to reject heat via convection. The model requires that the recirculation rate of the blowers be adjusted such that all the high quality waste heat is removed from the system.

A thermodynamic analysis was performed to determine the temperature and pressure at various states throughout the SOFC/heat exchanger system. Figure 4 shows the different numbered points identified where the state of the system will differ. In order to complete the analysis requiring as few iterations as possible, the temperature at points 8 and 11 for the hydrogen and oxygen systems must be specified. Similarly to the PEM system, the SOFC-based RFC system has a thermal enclosure which is being maintained at a constant temperature. The inlet gas at Point (PT) 1 is assumed to be at this enclosure temperature. It is assumed that the residence time of the gas in the closure is long enough for thermal equilibrium to exist between the reactant gases and their surroundings. The temperature at PT 2 for the hydrogen line is calculated by performing a mass and energy balance at PT 2 and assuming that the enthalpy, h, at each point $h \approx C_p T$.

$$T_2 = \frac{(\dot{m}_{H2} C_{p,H2} T)_1 + (\dot{m}_{H2} C_{p,H2} T)_{13} + (\dot{m}_{H2O} C_{p,H2O} T)_{13}}{(\dot{m}_{H2} C_{p,H2})_2 + (\dot{m}_{H2O} C_{p,H2O})_2} \tag{15}$$

The hydrogen mass flow rate at PT 1, $(\dot{m}_{H2})_1$, is the reactant consumption rate plus whatever small amount of reactant is lost due to venting or leakage. The hydrogen consumption rate, $\dot{m}_{H2,cons}$, in moles per second can be calculated for a given stack from the electrical power generated and average cell voltage.

$$\dot{m}_{H2,cons} = \frac{P_{ELE}}{2V_{CC}F_c} \tag{16}$$

P_{ELE} is the electrical power generated in W, V_{CC} is the average cell electrical potential of the fuel cell in V, and F_c is Faraday's constant, 96,485 Coulombs per mole. Note that stoiciometric oxygen flow is one half of the hydrogen flow in moles per second.

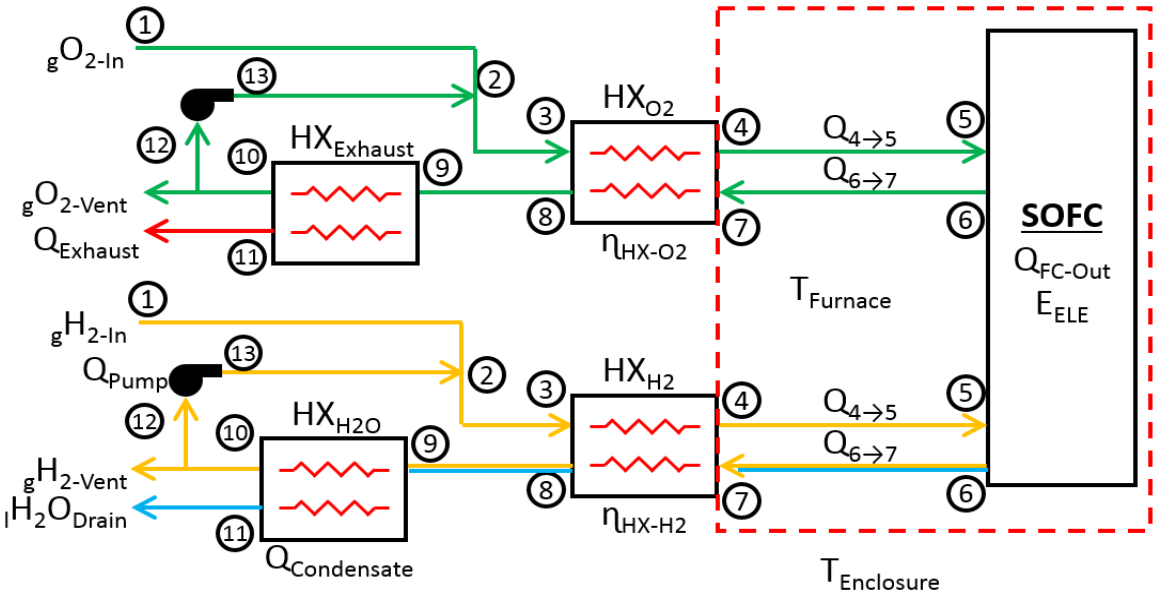

Figure 4. Solid oxide fuel cell schematic with breakdown of specific locations for thermodynamic analysis.

The specific heat of hydrogen and water at constant pressure, $C_{p,H2}$ and $C_{p,H2O}$, is extracted from property tables located in the model for a given fluid temperature T [9]. The hydrogen mass flow at PT13, $(\dot{m}_{H2})_{13}$,is the excess hydrogen recirculated through the loop to remove heat generated by the stack. This excess flow is calculated using a solver in Excel to allow the sum of the heat rejected in the heat exchangers (plus heat lost via conduction through the insulation) to equal the waste heat generated by the fuel cell. A small fraction of the steam in the hydrogen line will not be condensed and will also be recirculated. The effectiveness of the condenser is an input to the model which allows the quantity of water recirculated to be calculated.

$$(\dot{m}_{H2O})_{13} = (1 - \eta_{condenser})\dot{m}_{H2O,gen} \tag{17}$$

The quantity of water generated for a given stack is also calculated using Equation 16. The flow rates at PT 2 are simply the sum of the flow rate of hydrogen and water at PT 1 and PT 13. The same procedure is used to calculate the temperature of oxygen at PT 2, however, the calculation

is simpler since there is no water in the oxygen line. The trace level of impurities are ignored for these calculations.

The temperature at PT 3 is assumed to be equal to the temperature at PT 2. The hydrogen/water mixture temperature is denoted as the fuel temperature T_{fuel}. After passing through the recuperative heat exchanger the temperature at PT 4 of the fuel is described by Equation 18.

$$T_{fuel,4} = T_{fuel,3} + \frac{Q_{H2,3-4}}{(\dot{m}_{H_2} c_{p,H_2})_3} + \frac{Q_{H2O,3-4}}{(\dot{m}_{H_2O} c_{p,H_2O})_3} \quad (18)$$

The difference in C_p of hydrogen between points PT 3 and the average value between PT 3 and PT 4 is less than 1 percent, so this is a reasonable approximation. The difference in the specific heat of the water between PT 3 and the average value between PT 3 and PT 4 is around 4 percent, but water is only 15 percent of the molar fuel content and has a small impact on Equation 18. The oxygen temperature at PT 4 can be calculated using the same logic. The temperature at PT 5 is the operating temperature of the fuel cell, which is a known value. The allowable temperature rise of the gas is 25 °C which determines the temperature at PT 6. The temperature difference between PT 6 and PT 7 is also negligible. The temperature at PT 8 is an input and this allows for the calculation of the heat transfer through the heat exchanger. This determines the heat transfer between PT 3 and PT 4 because $Q_{3-4}=Q_{7-8}$.

$$Q_{7-8} = \dot{m}_{7-8} c_p (T_8 - T_7) \quad (19)$$

The mass flow from PT 7 to PT 8 is the inlet mass flow minus the quantity that is consumed by the fuel cell. The hydrogen line will also have the product steam generated that must be accounted for. The temperature doesn't change significantly between PT 8 and PT 9. The heat rejection from PT 9 to PT 10 is dependent on the effectiveness of the heat exchanger, η_{HX}, which is an input to the model.

$$T_{10} = T_9 + (1 - \eta_{HX})(T_9 - T_{11}) \quad (20)$$

The condensate temperature in the hydrogen condenser and the liquid water coolant temperature for the oxygen heat exchanger are inputs to the model and represent PT 11 for the hydrogen and oxygen systems, respectively. These temperatures at PT 11 were varied to optimize the mass and efficiency of the RFC. The temperature at PT 12 is equal to the temperature at PT 10. The temperature at PT 13 is calculated by assuming isentropic compression through the blower.

$$T_{13} = T_{12}\left[\left(\frac{P_{13}}{P_{12}}\right)^{\frac{\gamma-1}{\gamma}} - 1\right] + T_{12} \quad (21)$$

γ is the specific heat ratio of the gas, either oxygen or the hydrogen and water vapor mixture. Note that the specific heat ratio of the mixture is taken as the sum of each specific heat times its mole fraction. The operating pressure of the SOFC is assumed to be 101 kPa, and the only significant pressure drop in Figure 4 is through the fuel cell stack and each of the heat exchangers, which is an input to the model. This allows for the pressure to be calculated at every

point in Figure 4. Thus the ratio of the pressures at PT 13 and PT 12 can be input into Equation 21.

Knowing the temperature at each point in Figure 4 allows for the LMTD and heat transferred through each heat exchanger to be calculated. Thus the UA value for each heat exchanger can be calculated and the methods described for sizing the PEM heat exchanger are applicable to estimate the mass, volume, and heat transfer area required for the four heat exchangers.

Heat is rejected from the SOFC by recirculating the hydrogen and oxygen flow to remove heat from the stack and then rejected to the coolant in the second heat exchanger. The flow rate of gas required to remove the high quality heat is solved for using a goal seek in Excel to force the heat generated by the fuel cell to equal the heat lost to the surroundings plus the heat transferred in the recuperative heat exchangers. The power required to recirculate the reactant gases is one of the primary parasitic loads in the thermal system. For the hydrogen system the blower power, W_c, is calculated through Equation 22.

$$W_c = \frac{\dot{m}_{H2} c_{p,H2} T_{12}}{\eta_c}\left[\left(\frac{P_{13,H2}}{P_{12,H2}}\right)^{\frac{\gamma_{H2}-1}{\gamma_{H2}}} - 1\right] + \frac{\dot{m}_{H2O} c_{p,H2O} T_{12}}{\eta_c}\left[\left(\frac{P_{13,H2O}}{P_{12,H2O}}\right)^{\frac{\gamma_{H2O}-1}{\gamma_{H2O}}} - 1\right] \quad (22)$$

$P_{13,H2}$ is the partial pressure of hydrogen at PT 13, $P_{13,H2O}$ is the partial pressure of water vapor at PT 13, the same convention is used for the partial pressures at PT 12, and η_c is the efficiency of the mechanical blower. The same methodology is used to calculate the power consumed by the oxygen recirculation pump.

Further heat removal is required to condense the water in the hydrogen stream and to reduce the recirculating oxygen temperature. This heat is transferred to the liquid water coolant system used to cool the PEM EZ during EZ operation. The heat transferred to the coolant is then rejected in a heat exchanger within the radiator cold plate. The radiator for the SOFC is sized using the same method as for the PEM system.

The second thermal requirement in the SOFC RFC system is to reduce thermal cycling of the system components. For the PEM electrolyzer this is achieved via clever design of the second oxygen heat exchanger and designing for the temperature at PT 11 to be desired standby temperature of the EZ. The warm coolant at the exit is then directly routed to the EZ while it is not operating in order to keep it from cooling down while it is not operating. The SOFC is maintained at a desired standby temperature using electric heaters evenly distributed over the fuel cell. With a temperature difference between this standby temperature and the thermal enclosure temperature of several hundred degrees Celsius, the heater power lost from the fuel cell via radiation would be prohibitively large without any insulation and could potentially melt some of the ancillary components. Thus the SOFC is surrounded by a hermetic furnace for both thermal and external leakage purposes. The furnace consists of high temperature insulation and a hermetically sealed metal “hot box”. The heat loss for a given insulation thickness can be

calculated using thermal resistances. A planar geometry of SOFC was considered in this model so it was assumed that the thickness of the insulation was uniform in each direction.

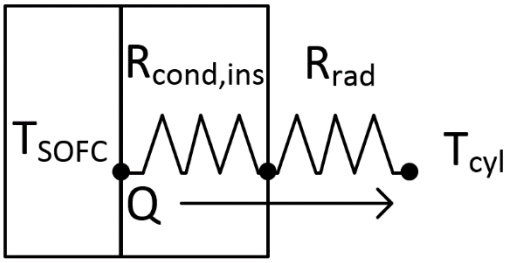

Figure 5. Thermal Circuit for solid oxide fuel cell (SOFC) heat transfer to controlled ambient environment.

The thermal resistance by conduction, R_{cond}, for a plane wall is a function of the thickness, t, of the insulation.

$$R_{cond} = \frac{t}{kA_{ins}} \tag{23}$$

The thermal conductivity, k, of high temperature Thermal Ceramics® TE 1800 Board and Shapes Molded Min-k insulation was used. A_{ins} is the cross sectional area of the insulation. The thickness t was optimized to overall system efficiency which is achieved via minimizing the heater power required during standby but also interestingly minimizing the power of the recirculating hydrogen and oxygen blowers during fuel cell operation. The heater power tends to be the dominant factor in this optimization. Since there are six sides of the fuel cell there are size parallel heat paths for conduction and the heat paths must be summed accordingly to calculate an overall conduction resistance through the insulation.

$$R_{cond,tot} = \frac{1}{\sum_{i=1}^{6} \frac{1}{R_{cond,i}}} \tag{24}$$

After optimizing for the thickness the heat loss, $Q_{FC\text{-}ins}$, from the fuel cell to the hermetic box (also the temperature of the outside surface of the insulation) can be calculated.

$$Q_{FC-ins} = \frac{T_{SOFC} - T_{ins}}{R_{cond,tot}} \tag{27}$$

Note that the PEM FCs and EZ were also insulated with low temperature insulation using the same methods. After conducting through the insulation, the heat will radiate to the thermal enclosure [3].

$$R_{rad} = \frac{1}{h_r A_{ins}} \tag{25}$$

$$h_r = \varepsilon\sigma(T_s + T_{sur})(T_s^2 + T_{sur}^2) \tag{26}$$

A_{ins} is the outside surface area of the insulation and σ is the Stefan-Boltzmann constant, 5.67×10^{-8} W/m^2-K^4. The emissivity, ε, of a ceramic fiber was assumed to be 0.7. T_s is the

exterior surface temperature of the insulation which was calculated by assuming a 20 K temperature differential between the furnace and the enclosure. T_{sur} is the temperature of the surroundings which in this case is the controlled temperature of the enclosure, a known quantity. The radiation heat leak into the thermal enclosure from the FC and EZ is part of the energy balance that determines the heater power required or the heat removal requirements to maintain the enclosure temperature.

TRADE STUDY RESULTS

For a PEM RFC a deionized water coolant system is able to reject heat from the operating components (FC or EZ) while maintaining the temperature of the other components in standby mode. A radiator was sized to reject waste heat generated by the PEM FC. The primary parasitic electrical loads for the PEM thermal system is the coolant pump. Major contributors the mass of the PEM thermal system include the radiator, coolant, and coolant tank. Figure 6 shows the mass breakdown of a PEM based RFC system by subsystem for the Martian Equator. Note that the thermal management system accounts for nearly 50 % of the total system mass. The radiator is the heaviest element of the thermal control system (TCS).

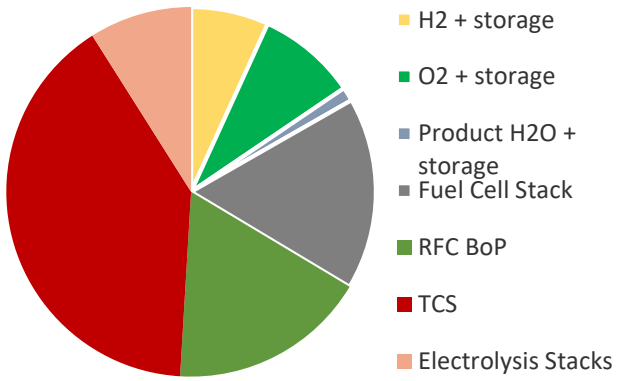

Figure 6. Mass breakdown by subsystem including hydrogen (H2) plus storage tanks, oxygen (O2) plus storage tanks, product water (H2O) plus storage tanks, fuel cell stacks, regenerative fuel cell (RFC) fluidic balance of plant (BoP), thermal control system (TCS), and electrolysis stacks for a Proton Exchange Membrane fuel cell based RFC at the Martian Equator.

The SOFC thermal system has a coolant pump as a parasitic load but also high temperature blowers to recirculate reactants to reject heat from the fuel cell stack. While the fuel cell is in standby mode during electrolysis the electric heaters to maintain the SOFC at a desired temperature is also a significant parasitic load. In addition to mass burdens of the PEM system the SOFC also has four heat exchangers that must be considered. High temperature insulation is also required to prevent thermal cycling of the SOFC. This additional heat exchanger and insulation mass and also mass from the hermetic box tend to make SOFC RFCs a heavier option than PEM FCs; however, the SOFC systems tend to be more efficient than their PEM counterparts. This higher efficiency results in a smaller radiator that is required and this is

reflected by the TCS taking up a much percentage of the total RFC mass, shown in Figure 7 for a SOFC based RFC at the Martian Equator. Another reason for the TCS only accounting for around 20 percent of the total mass is that the high temperature insulation and hermetic enclosure were grouped into the fuel cell stack category which thus makes the fuel cell stack masses much more significant.

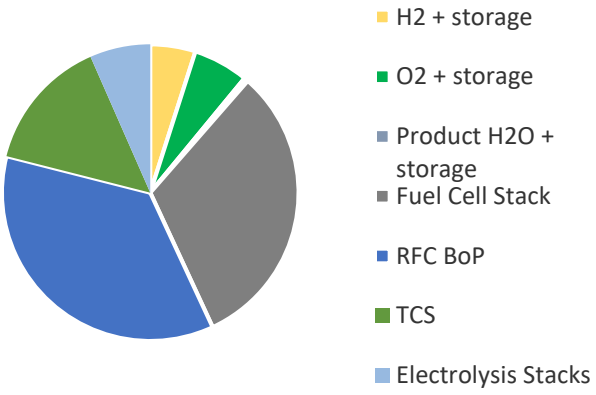

Figure 7. Mass breakdown by subsystem including hydrogen (H2) plus storage tanks, oxygen (O2) plus storage tanks, product water (H2O) plus storage tanks, fuel cell stacks, regenerative fuel cell (RFC) fluidic balance of plant (BoP), thermal control system (TCS), and electrolysis stacks for a Proton Exchange Membrane fuel cell based RFC at the Martian Equator. Note that the high temperature insulation and hermetic enclosure mass are included in the fuel cell stack category and not the TCS.

The initial trade study results strongly indicated that, although the base thermodynamic advantages of solid oxide fuel cell technology are encouraging, there are still many details requiring further development to implement solid oxide fuel cell technology for an aerospace application. For all mission locations, PEM fuel cells showed an overall advantage when considering the weighting criteria in **Error! Reference source not found.**3. Each criterion was identified as being maximized or minimized to reflect the most advantageous configuration. For those criteria that were maximized, Equation 27 was used. In Equation 27, a positive number reflected an advantage in PEM technology, while a negative number reflected an advantage in solid oxide technology.

$$Normalized\,Value = WeightFactor*(PEM - SolidOxide)/[(PEM + SolidOxide)/2] \quad (27)$$

For criteria that needed to be minimized, Eq. 27 was used but a multiplier of -1.0 was applied to the normalized value. Again, a positive number reflected an advantage in PEM technology, while a negative number reflected an advantage in solid oxide technology. To avoid perception bias, color-coding was used to note the advantage in the results table, rather than a positive or negative number value. The results for each mission can be seen in Table 3, where PEM advantages are colored in blue and noted by the abbreviation “PEM” while solid oxide advantages are colored in orange and noted by the abbreviate “SOFC”. Ties are noted in purple.

To show the relative difference between solid oxide fuel cell-based RFC systems and PEM fuel cell-based RFC systems for each mission location, the total system mass is shown in Figure 8, and total system volume is shown in Figure 9. The photovoltaic charge power required is shown in Figure 10. The system specific energy is shown in Figure 11.

Table 1. RFC Trade Study Performance Metric Results for All Mission Locations.

Performance Metric	**Weight Factor**	**Parameter Intent**	**Mars Equator**	**Mars Mid-Latitude**	**Moon Equator**	**Moon South Pole**
RFC System Mass	0.5	Minimize	0.19 (PEM)	0.16 (PEM)	0.08 (PEM)	0.14 (PEM)
RFC System Volume	0.25	Minimize	0.01 (PEM)	0.01 (PEM)	0.0 (tie)	0.0 (tie)
PV Charge Power Required	1.0	Minimize	0.05 (PEM)	0.02 (PEM)	0.05 (PEM)	0.06 (SOFC)
Specific Energy	0.5	Maximize	0.10 (PEM)	0.08 (PEM)	0.01 (SOFC)	0.06 (PEM)
Weighted Total Value			**0.36 (PEM)**	**0.26 (PEM)**	**0.12 (PEM)**	**0.13 (PEM)**

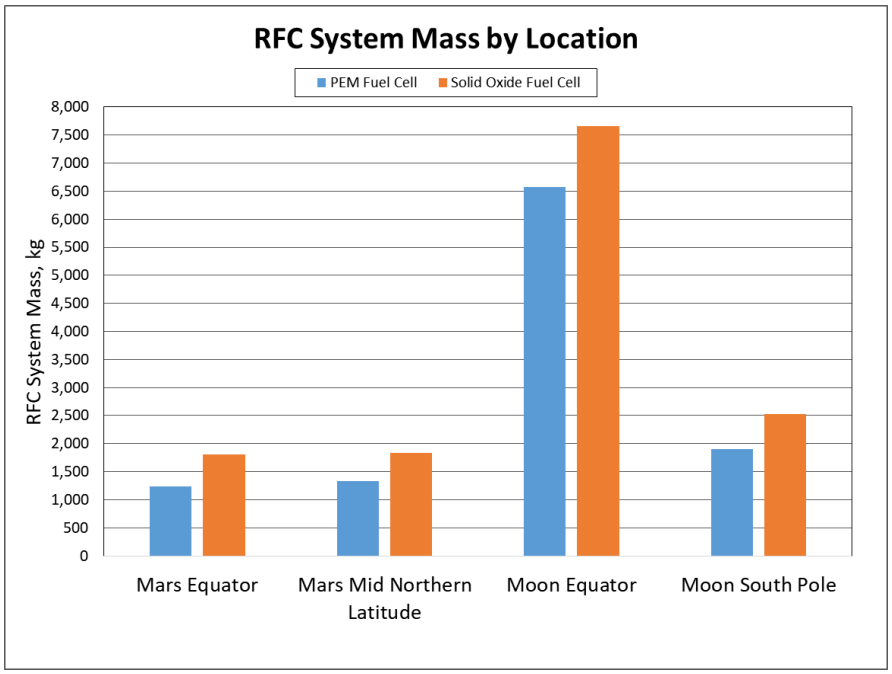

Figure 8. RFC System Mass by Location. PEM fuel cell-based RFC system mass is shown in blue, while solid oxide fuel cell-based RFC system mass is shown in orange. Both fuel cell architectures utilize a PEM electrolysis stack.

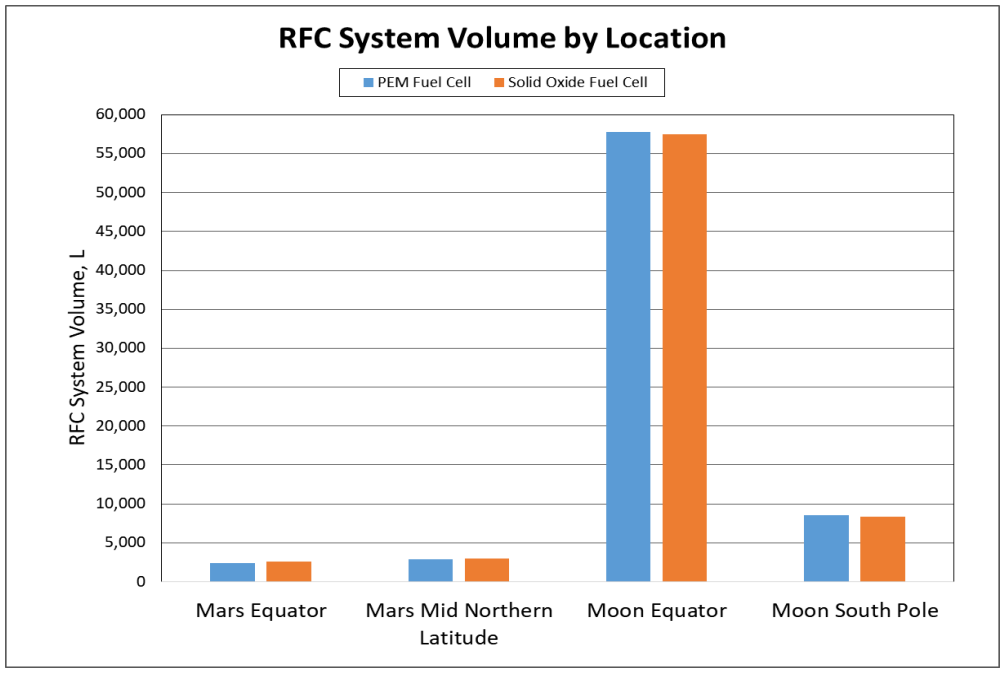

Figure 9. RFC System Volume by Location. PEM fuel cell-based RFC system volume is shown in blue, while solid oxide fuel cell-based RFC system volume is shown in orange. Both fuel cell architectures utilize a PEM electrolysis stack.

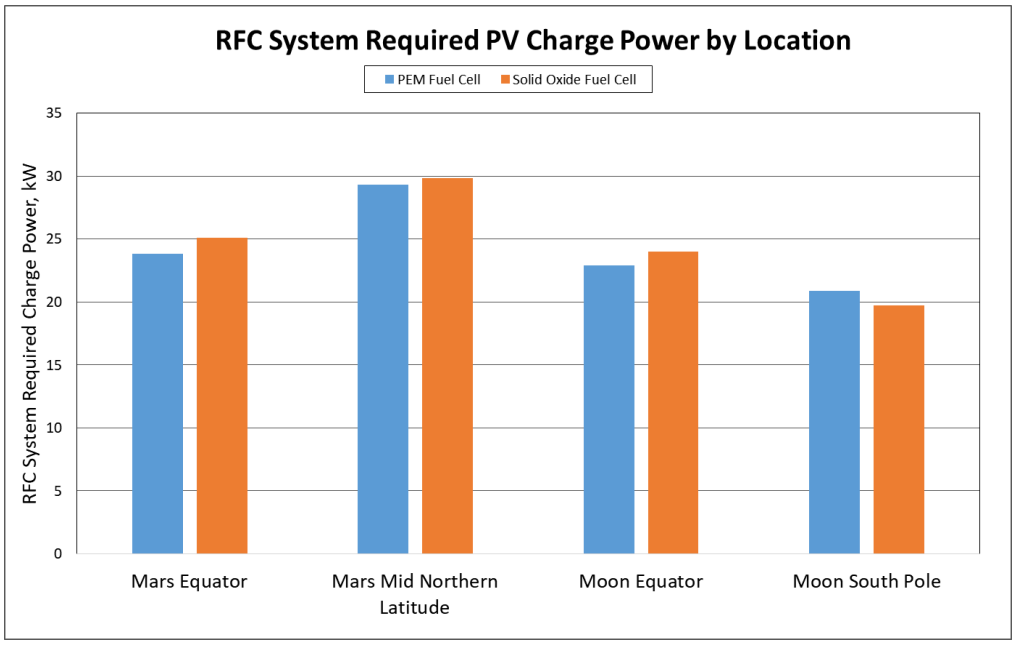

Figure 10. RFC System PV Charge Power by Location. PEM fuel cell-based RFC system PV charge power is shown in blue, while solid oxide fuel cell-based RFC system PV charge power is shown in orange. Both fuel cell architectures utilize a PEM electrolysis stack. PV charge power, or Photovoltaic array charge power, indicates the amount of solar energy needed for RFC operation during the daytime cycle.

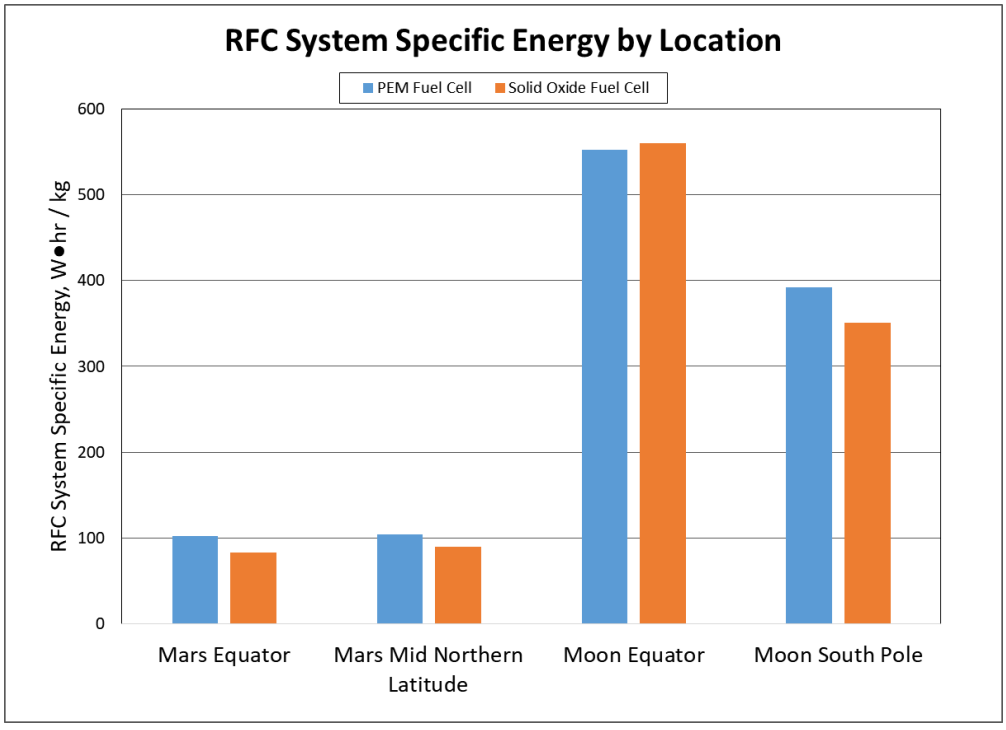

Figure 11. RFC System Specific Energy by Location. PEM fuel cell-based RFC system specific energy is shown in blue, while solid oxide fuel cell-based RFC system specific energy is shown in orange. Both fuel cell architectures utilize a PEM electrolysis stack.

For all mission locations, PEM fuel cells emerged as the most advantageous fuel cell technology for a near-term application that meets the surface power requirements. For lunar locations, the trade is closer, as the long nighttime durations make electrolysis the critical RFC component. In particular, the lunar South Pole requires further analysis to investigate the appropriate operating concept for electrolysis. The higher efficiency of solid oxide fuel cells is also more apparent for the lengthy lunar daytime durations. However, the higher system mass, volume, and parasitic power required for the solid oxide fuel cell makes the PEM fuel cell the best overall technology.

NOMENCLATURE

A	heat transfer area
A_{ins}	heat transfer area of insulation
A_R	radiator area
c_p	specific heat at constant pressure
d	diameter of heat exchanger tubes
D	diameter of coolant vessel
E	weld joint efficiency factor in pressure vessel
F	view factor
F_c	Faraday's constant, 96,485 Coulombs per mol
k	thermal conductivity
L	length of coolant vessel
L_{HX}	heat exchanger length
$LMTD$	log mean temperature different
L/D	length to diameter ratio of coolant vessel
m_{HX}	heat exchanger mass
m_R	radiator mass
$\dot{m}$	mass flow rate

$\dot{m}_{coolant}$	coolant mass flow
n_t	number of tubes used in heat exchanger
n_p	number of passes within a heat exchanger
n_s	number of stacked tubes within heat exchanger
P	pressure
P_{ELE}	electrical power generated by fuel cell
Q	heat transfer
Q_{FC}	waste heat generated by fuel cell
R_{cond}	thermal resistance by conduction
$R_{cond,tot}$	total thermal resistance by conduction
R_{cyl}	radius of coolant vessel
R_{rad}	thermal resistance by radiation
S	safety factor for pressure vessel
t_{cyl}	coolant vessel thickness in cylinder section
t_{head}	coolant vessel thickness in head section
t_{HX}	heat exchanger thickness
t_R	radiator thickness
T_{BP}	radiator baseplate temperature
T_s	exterior surface temperature of fuel cell insulation
T_{sink}	ambient sink temperature for radiator
T_{sur}	temperature of thermal enclosure
U	overall heat transfer coefficient
V	coolant vessel volume
V_{CC}	average cell electrical potential of fuel cell
w_{HX}	heat exchanger width

$\dot{W}_{actual}$	actual power required to pressurize a fluid
$\dot{W}_{ideal}$	ideal power required to pressurize a fluid
WR	weight ratio of heat exchanger weight to heat transfer area
ε	emissivity of radiator
γ	specific heat ratio
ΔP	change in pressure of a fluid
ΔT	*temperature differential*
ΔT	temperature difference between baseplate and radiator
$\eta_{condensor}$	condenser efficiency
η_{HX}	heat exchanger effectiveness
η_{pump}	pump efficiency
ρ	fluid density
$\rho_{carbonsteel}$	density of carbon steel
ρ_{HX}	density of heat exchanger material
ρ_R	density of radiator material
σ	Stefan-Boltzmann constant

SUBSCRIPTS

c	cold fluid within a heat exchanger
cons	consumed
fuel	hydrogen and steam mixture
gen	generated

h hot fluid within a heat exchanger

H_2	hydrogen
H_2O	water

i	inlet to a heat exchanger
ins	insulation
o	outlet of a heat exchanger
O_2	oxygen

ACRONYMS

EZ	Electrolyzer
FC	Fuel Cell
NASA	National Aeronautics and Space Administration
PEM	Proton Exchange Membrane
SOFC	Solid Oxide Fuel Cell

REFERENCES

1. EG&G Technical Services, Inc. *Fuel Cell Handbook, Seventh Edition.* U.S. Department of Energy Office of Fossil Energy. National Energy Technology Laboratory. November 2004.
2. Fowler, Michael. "Degradation and Reliability Analysis of PEM Fuel Cell Stacks."
3. Incropera, Dewitt, Bergman, and Lavine. *Fundamentals of Heat and Mass Transfer.* Wiley. 2013.
4. "Typical Overall Heat Transfer Coefficients (U – Values)." Engineering Page. <http://www.engineeringpage.com/technology/thermal/transfer.html>.
5. Fraas, Arthur. *Heat Exchanger Design*. Wiley, 1965.
6. Colozza, Anthony and Kenneth Burke. "Evaluation of a Passive Heat Exchanger Based Cooling system for Fuel Cell Applications." NASA/TM 2011-216962.
7. Metcalf, Kenneth. "Power Management and Distribution (PMAD) Model Development." NASA/CR- 2011-217268.
8. 2013 ASME Boiler and Pressure Vessel Code. VIII Rules for Construction of Pressure Vessels. Division 1.
9. National Institute of Standards and Technology (NIST). Reference Fluid Thermodynamic and Transport Properties (REFPROP) Database.